Peer-reviewed version available at *Energies* **2018**, *11*, 204; doi:10.3390/en11010204

Article

Performance Study of a Cylindrical Parabolic Concentrating Solar Water Heater with Nail Type Twisted Tape inserts in the Copper Absorber Tube

Amit K Bhakta [1,*], Nitesh K Panday [2] and Shailendra N Singh [2]

[2] Heat Transfer Laboratory, IIT (ISM) Dhanbad-826004, India; nitesh.panday72@gmail.com
[3] Heat Transfer Laboratory, IIT (ISM) Dhanbad-826004, India
* Correspondence: jgecbitsismd@gmail.com; Tel.: +91-9933038687

Abstract: This paper reports the overall thermal performance of a cylindrical parabolic concentrating solar water heater (CPCSWH) with inserting nail type twisted tape (NTT) in the copper absorber tube for the nail twist pitch ratios 4.787, 6.914 and 9.042 respectively. The experiments are conducted for a constant volumetric water flow rate and during the time period 9:00 h to 15:00 h. The useful heat gain, hourly solar energy collected and hourly solar energy stored of this solar water heater are found higher for nail twist pitch ratio 4.787. The above said parameters are found to be a peak at noon and observed to follow the path of variation of solar intensity. At the starting of the experiment, the value of charging efficiency is observed to be maximum. Whereas the maximum value of instantaneous efficiency and overall thermal efficiency are observed at noon. The key finding is that the nail twist pitch ratio enhances the overall thermal performance of the CPCSWH.

Keywords: cylindrical parabolic reflector; nail twist pitch ratio; water storage tank; thermal efficiency; solar energy collected.

1. Introduction

At present era utilization of solar energy increases with the development of societies as well as the development of solar energy collected techniques. CPCSWH is one of these techniques which are extensively used in the fields of power generation and some chemical processing industries due to it has few favorable characteristics, such as high temperature (ranges up to 400^{o}C) can be obtained due to its higher concentration ratio, easy to maintenance, compact size, and simple design. Huang et al. [1] used a black liquid as working fluid and investigated the thermal performance of cylindrical parabolic solar collector. They found better thermal performance using black liquid. Heiti and Thodos [2] compared the instantaneous efficiency obtained with and without coated absorber tube. Their results showed the better instantaneous efficiency for the coated absorber tube. Hamad [3] studied the influence of water mass flow rate on the instantaneous efficiency of the cylindrical parabolic solar concentrator. Their result showed that instantaneous efficiency increases with increasing of water mass flow rate. Mullick and Nanda [4] numerically studied the variation of heat loss factor with absorber tube temperature and absorber diameter. Their results showed that heat loss factor positively changes with absorber tube temperature. Kothdiwala et al. [5] studied the influence of tracking and longitudinal configuration of the compound parabolic concentrating solar collector on the thermal performance. Eskin [6] presented temperature variation of absorber, glass envelope and water outlet. Eck and Hirsch [7] conveyed the experimental investigation of a parabolic trough based power generation plant. Kim et al. [8] numerically and experimentally studied the thermal performances of an evacuated compound parabolic concentrator. They compared the experimental results with the numerical results and their results showed that the thermal performance of CPC in tracking mode much higher than the same obtained from the non-tracking mode. Oommen and Jayaraman [9] conducted an experiment on a compound parabolic concentrating collector to study the steam generation and solar energy collection. Fadar et al. [10] studied the adsorption refrigeration system run by parabolic trough collector. Padilla et al. [11] studied the heat loss and collector efficiency numerically. Gang et al. [12] performed the experimental investigation on exergy efficiency and overall thermal efficiency of the compound parabolic collector. Kumaresan et al. [13] studied the overall heat loss coefficient of the storage tank, charging efficiency and overall performance of Parabolic Trough Collector experimentally. Their results showed that the charging efficiency is maximum at the beginning of the experiment and overall thermal efficiency increases with hourly solar energy stored. Reddy [14] studied the performance of solar parabolic trough power plant. Ceylan and Ergun [15] conducted the experimental study on a temperature controlled CPC and reported energy efficiency and exergy efficiency. Jafar and Sivaraman [16] conducted experiment on parabolic trough collector to study the influence of nail twisted tape (twist ratio 2 and 3) on thermo-hydraulic performance using Al_2O_3/water nanofluid. Their results showed that heat transfer far better for twist ratio 2. Mwesigye et al. [17] investigated the entropy generation caused by fluid friction and heat transfer in the receiver tube. Khanna and Sharma [18] showed the circumferential temperature distribution of the absorber tube of a CPC. Jaramillo et al. [19] found that the thermal performance significantly improves with twisted tape inserts in the absorber tube. Liang et al. [20] used Monte Carlo Method analyze the solar flux distribution on the receiver and optical thermal performance of the parabolic trough collector. Fuqiang et al. [21] investigated and compared the overall heat transfer and thermal strain of the copper absorber tube. Bortolato et al. [22] used a flat bar and plate absorber instead of the circular absorber and they found overall thermal efficiency significantly improved. Zhao et al. [23] used Monte Carlo Ray Trace method and their result showed that the circumferential heat flux distribution on the receiver tube. Zou et al. [24] theoretically studied the optical performance of the parabolic trough solar collector. Fraidenraich et al. [25] studied the angular acceptance function of a cylindrical parabolic collector.

From the above literature survey, it has been observed that most of the researchers have worked on the cylindrical parabolic collector with the plain absorber tube and they determined the thermal performances only. Very few researchers have worked on the parabolic trough collector with inserts the nail twisted tape in the absorber tube and they studied only the hydraulic performance parameters. No researcher studied the thermal performance of the CPCSWH with the inserting NTT in the absorber tube. In the present experimental study, the influence of a new parameter, namely, nail twist pitch ratio on the thermal performance is reported. The main objectives are concentrated to study the influence of nail twist pitch ratio on useful heat gain, hourly solar energy collected and hourly energy stored with the time of the day.

2. Experimental setup and procedure

2.1 Description of the experimental set up and experimental procedure

Details of the CPCSWH experimental setup have been shown by a schematic diagram (Figure 1). The schematic of sectional views (front view and side view) of nail type twisted tape insert in the absorber tube have been shown in Figure 2. Figures 3 and 4 show the photographic view of the CPCSWH experimental setup (manufactured by Ecosense Sustainable Solutions Pvt. Ltd., Model: EcoSCTS-2.1) and NTT respectively. The CPCSWH consists of a water storage tank (capacity 28 litres), circulating pump, parabolic concentrating reflector (PCR) and copper absorber tube. The PCR made of Acrylic mirror with a highly reflecting surface of reflectivity 0.90 and its focal length is 0.6065 m (rim angle 67.24˚). It has a reflecting surface which consists of parabolic mirrors of 1.018 m^2 aperture area, each (0.834 m width and 1.220 m length), with a total aperture area of 2.036 m^2, which concentrates the incoming solar beam radiation to the absorber tube with concentration ratio 20.598. The copper tube is used as a solar radiation receiver with absorptance is 0.95, which is placed along the focus axis of the concentrating reflector. It is coated with the black-nickel coating, and is covered by a glass envelope to minimize heat losses through convection and conduction. Glass envelope has the dimension of inner diameter 0.066 m and outer diameter 0.071 m with transmissivity 0.85. The rubber corks are incorporated at the ends of the glass envelope to achieve an air-tight enclosure. The

Preprints (www.preprints.org) | NOT PEER-REVIEWED | Posted: 5 December 2017 doi:10.20944/preprints201712.0030.v1

Peer-reviewed version available at *Energies* **2018**, *11*, 204; doi:10.3390/en11010204

main function of the absorber tube of a CPCSWH is to absorb the concentrated solar radiations and transfer the concentrated solar radiation to the water flowing through it. A pump pumps water to flow continuously through the absorber tube of the CPCSWH to the water storage tank and during the flow through the absorber tube absorbed solar energy transfer takes place from absorber tube to flowing water. A pump regulating knob is used to control the volumetric water flow rate (in litre/min). A water flow sensor (Sea, model: YF-S201) is fitted in line with the Hydraulic Hose pipe (between the pump's outlet and the inlet of the absorber tube) to measure the volumetric water flow rate. Hydraulic Hose pipes are connected between the pump and water flow sensor, water flow sensor and absorber tube inlet, and absorber tube outlet and the water storage tank. The water storage tank is made of Stainless Steel material and cylindrical in shape. The water storage tank is insulated with glass wool and covered by a thick black colour Rexene to prevent heat losses and placed at the bottom of the cylindrical parabolic reflector. The thermocouples are inserted on the surface of the absorber tube, inside the water storage tank, water storage tank inlet as well as at the inlet and outlet of the absorber tube to measure the water temperatures on same locations. A display board equipped with five numbers of digital temperature indicator (connected with the above-mentioned thermocouple) to indicate the thermocouple's deflection (i.e., temperature readings) and a water flow rate indicator (connected with water flow sensor) to indicate the volumetric water flow rate. During the experiment temperatures and water flow rate are recorded from the display board. Two pressure transducers (Setra, model: 3100) have been used in order to measure the pressure at outlet and inlet of the absorber tube. One is placed in the inlet of the absorber tube and the other one is placed at the outlet of the absorber tube. The tracking mechanism consists of an embedded electronic control system. The electronic control system equipped with Light Dependent Resistor (LDR) to move the collector with the apparent motion of the Sun so that solar radiation incident on collector aperture at 90^{o} angle. The PCR rotates around the horizontal North-South axis to track the Sun as it moves through the sky during the day. The solar intensity is recorded by a Pyranometer connected with a Solar Power Meter (Tenmars TM-207).

Initially, the experiment is conducted with plain copper absorber tube and next experiments are conducted with inserting the NTT in the absorber tube one by one with varying nail twist pitch ratios (4.787, 6.914 and 9.042). Aluminium strips are used to manufacture the twisted tape and MS headless screws are inserted into the previously drilled holes at a twist pitch distance over the length of the twisted tape. The experiment was started from 25^{th} April of 2017 to June of 2017 and during the time period from 09:00 h to 15:00 h and the experimental works have been conducted at IIT(ISM) Dhanbad (Latitude 23 ^{o}47″ N and Longitude 86^{o} 30″ E), a city situated in the east-northern region of India (Country) with an elevation of 232.0 m (approx.) above from the mean sea level (MSL).

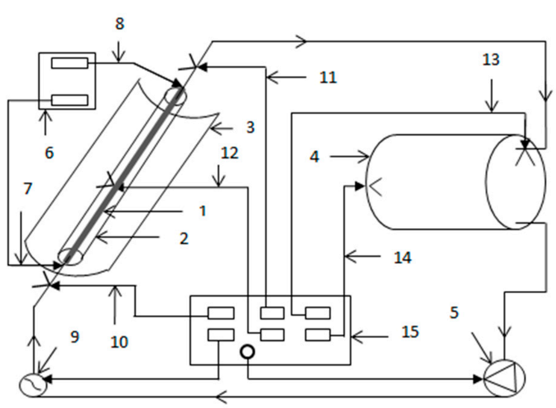

1. Copper absorber tube, 2. Glass envelope, 3. Parabolic concentrating Reflector, 4. Water storage tank, 5. Pump, 6. Digital pressure indicator, 7. & 8. Pressure transducers, 9. Water flow sensor, 10, 11, 12, 13 & 14. Thermocouples, 15. Display board

Figure 1. The schematic diagram of the CPCSWH experimental setup.

Preprints (www.preprints.org) | NOT PEER-REVIEWED | Posted: 5 December 2017 doi:10.20944/preprints201712.0030.v1

Peer-reviewed version available at Energies 2018, 11, 204; doi:10.3390/en11010204

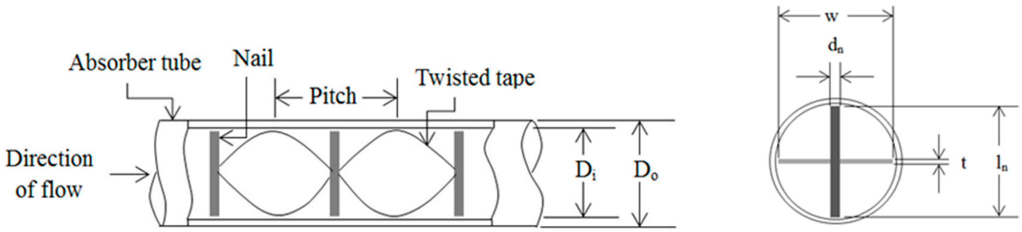

Figure 2. Schematic sectional views of NTT.

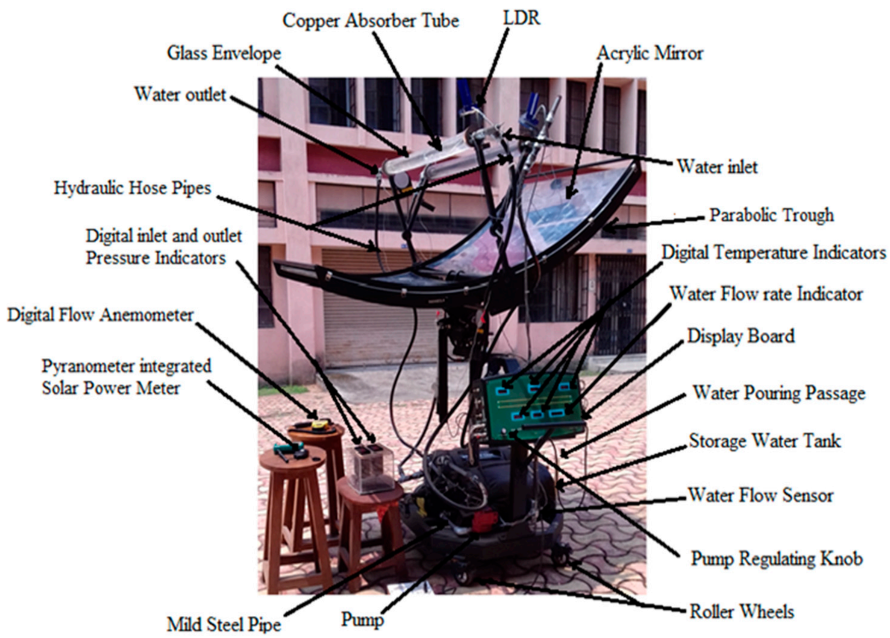

Figure 3. Photographic view of CPCSWH experimental setup.

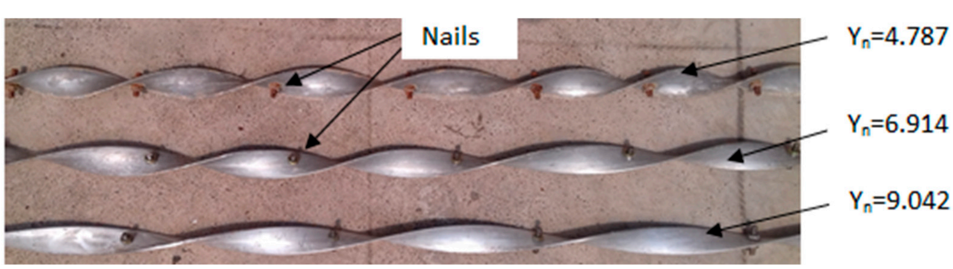

Figure 4. Photographic view of NTT.

2.2 The specifications of the CPCSWH experimental set up and (NTT) have been shown in Tables 1.

Table 1. Specifications of the CPCSWH experimental setup and NTT.

Preprints (www.preprints.org) | NOT PEER-REVIEWED | Posted: 5 December 2017 doi:10.20944/preprints201712.0030.v1
Peer-reviewed version available at Energies 2018, 11, 204; doi:10.3390/en11010204

Sl. No.	Parameter	Value
1	Reflector aperture area	2.036 m^2
3	Length of absorber tube	1.220 m
4	Inner diameter of absorber tube	0.023 m
5	Outer diameter of absorber tube	0.025 m
6	Width of NTT	0.020 m
7	Thickness of NTT	0.0012 m
8	Length of nail	0.020 m
9	Diameter of nail	0.004 m
10	Effective length of nail	0.0188 m

3. Data reduction

The experimental data are used in the below equations to meet experimental results
Water mass flow rate is calculated using equation (1) as follows

$$m=\rho_f V_f , \tag{1}$$

Useful heat gain is the solar energy absorbed by the circulating water during the flow through absorber tube and is calculated using the equation (2) as follows

$$Q=mc_p\left(T_o - T_i\right), \tag{2}$$

Bulk mean temperature is calculated using the equation (3) as follows

$$T_b=\frac{T_i+T_o}{2}, \tag{3}$$

Bulk mean temperature of the water in the water storage tank is calculated using the equation (4) as follows

$$T_{b,st}=\frac{T_{st,j+1}+T_{st,j}}{2}, \tag{4}$$

Hourly solar energy collected is the solar energy gain during the one hour time interval as given by Kumaresan et al. [13] and it is calculated using equation (5) as follows

$$E_c=\left[\frac{mc_p\left(T_o - T_i\right)_{j+1}+mc_p\left(T_o - T_i\right)_j}{2}\right]\times 3600, \tag{5}$$

Hourly solar energy stored is the solar energy stored in the water storage tank during the one hour time interval as given by Kumaresan et al. [13] and it is calculated using equation (6) as follows

$$E_{st}=m_{st}c_{p,st}\left(T_{st,j+1} - T_{st,j}\right), \tag{6}$$

Temperature rise parameter is calculated using the equation (7) as follows

$$TRP=\frac{T_o - T_i}{I_b}, \tag{7}$$

Preprints (www.preprints.org) | NOT PEER-REVIEWED | Posted: 5 December 2017 doi:10.20944/preprints201712.0030.v1

Peer-reviewed version available at Energies 2018, 11, 204; doi:10.3390/en11010204

Instantaneous efficiency is calculated using equation (8) as follows

$$\eta_i = \frac{mc_p(T_o - T_i)}{A_{ap} I_b}, \tag{8}$$

Charging efficiency is ratio of hourly solar energy stored in the water storage tank to hourly solar energy collected as given by Kumaresan et al. [13]. It is calculated using equation (9) as follows

$$\eta_{ch} = \frac{E_{st}}{E_c}, \tag{9}$$

Overall system efficiency is the ratio of hourly solar energy stored in the water storage tank to hourly solar energy incident on the parabolic concentrating reflector. It is calculated using equation (10) as follows

$$\eta_o = \frac{E_{st}}{A_{ap} I_h}, \tag{10}$$

4. Uncertainty analysis

The method proposed by Kline and McClintock [26] is used for uncertainty calculation. In the experimental measurements the maximum value of uncertainties is found to be ± 3.711 % for useful heat gain, ± 3.48 % for hourly solar energy collected, ± 0.703 % for hourly solar energy stored, ± 1.649 % for temperature rise parameter, ± 3.134 % for instantaneous efficiency, ± 5.99 % for charging efficiency and ± 0.76 % for overall thermal efficiency. The accuracies of the instruments have been used for uncertainty analysis are shown in table 2.

Table 1. Accuracies of the instruments.

Sl. No.	Instruments	Accuracy
1	Water Flow Sensor (Sea, model : YF-S201)	± 10 %
2	Digital Anemometer (model: AVM -03)	± 3 % (for wind velocity) ± 2 °C (for temperature)
3	Pyranometer integrated with Solar Power Meter (model: TM-207)	± 0.499 %
4	Thermocouple	± 0.4 %
5	Pressure transducer (Setra, model: 3100)	± 0.25 %

5. Result and discussion

5.1 Solar intensity with time

Figure 5 presents the variation of solar intensity with time. From this figure, it is very clear that slope of solar intensity increases from 9:00 h to 11:00 h and after that its slope increases slowly up to noon. The peak values of solar intensity are observed at 12:00 h. After 13:00 h, the value of solar intensity starts to reduce with a higher decreasing rate till 15:00 h.

Preprints (www.preprints.org) | NOT PEER-REVIEWED | Posted: 5 December 2017 doi:10.20944/preprints201712.0030.v1

Peer-reviewed version available at Energies 2018, 11, 204; doi:10.3390/en11010204

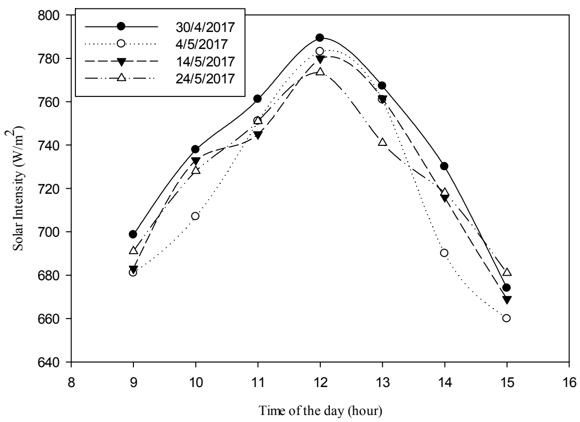

Figure 5. Variation of solar intensity with time of the day.

5.2 Effect of nail twist pitch ratio on useful heat gain

Figure 6 shows the variation of useful heat gain with time for plain absorber tube and absorber tube with NTT inserts. The useful heat gain changes progressively with time from 9:00 h to 12:00 h and then starts to deteriorate from 12:00 h to 15:00 h as shown in Figure 6. The useful heat gain is maximum at noon when solar intensity is maximum. The variation of useful heat gain follows the path of variation of solar intensity. Also useful heat gain increases for smaller nail twist pitch ratio. This is owing to the fact of swirl flow and turbulence induced by the NTT. Also with smaller nail twist pitch ratio tape twist pitch decreases and no. of nail increases that in turn intensifies swirling and turbulence deeply. The combined effect increases in heat transfer time and rate of heat transfer from absorber tube to flowing circulating water. Due to this useful heat gain increases. In the present experimental study, the maximum useful heat gain increases by 12.462% for nail twist pitch ratio 4.787, 10.753% for nail twist pitch ratio 6.914 and 7.591% for nail twist pitch ratio 9.042 than useful heat gain obtained from the plain absorber tube. Therefore useful heat gain obtained from the absorber tube with inserts NTT is found much higher than that in the plain absorber tube.

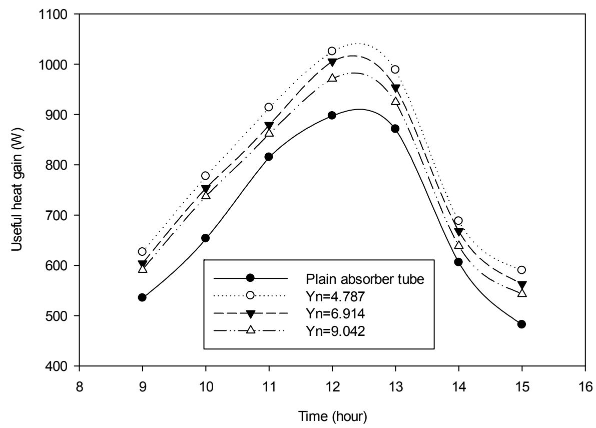

Figure 6. Variation of useful heat gain with time and nail twist pitch ratio

5.3 Effect of nail twist pitch ratio on water outlet temperature and water temperature in the water storage tank

Figures 7 and 8 indicate the variation of the water outlet temperature and water temperature in the water storage tank with time for different nail twist pitch ratios (4.787, 6.914 and 9.042). These

 doi:10.20944/preprints201712.0030.v1

Peer-reviewed version available at *Energies* **2018**, *11*, 204; doi:10.3390/en11010204

figures clearly show that water outlet temperature and water temperature in the water storage tank both changes positively with a higher incremental rate from 9:00 h to 12:00 h as solar intensity increases during this time period. From 12:00 h to 15:00 h water outlet temperature and water temperature in the water storage tank both increases slowly and NTT insert absorber tube improves these temperature results. This is due to the fact that the stored water is flowing through the absorber tube to water storage tank and from water storage tank to the absorber tube i.e., a closed loop system and hot water stored in the water storage tank is entering the absorber tube to absorb the concentrated solar energy from the absorber tube. Neither fresh water entering into the system nor energy withdrawing from the system. Stored hot water is being heated again and again only during the experiment. Also, the water outlet temperature of increases for NTT inserts absorber tube with smaller nail twist pitch ratio. As swirl flow and turbulent created by tape twist and nail of the NTT inserts absorber tube. Also, the water temperature in water storage tank is affected by the same influences of the NTT. During the experiment, the maximum water outlet temperature has found to be 77.170 ^{o}C for nail twist pitch ratio 4.787 at 15:00 h. Therefore, it is very transparent that the water temperature in the water storage tank follows the path of variation of circulating water temperature at the outlet of absorber tube.

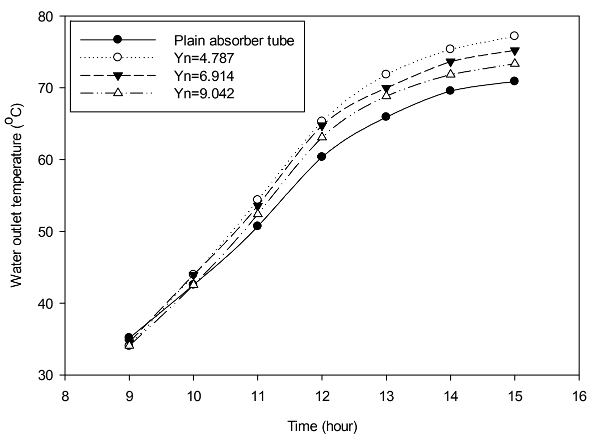

Figure 7. Variation of water outlet temperature with time and nail twist pitch ratio

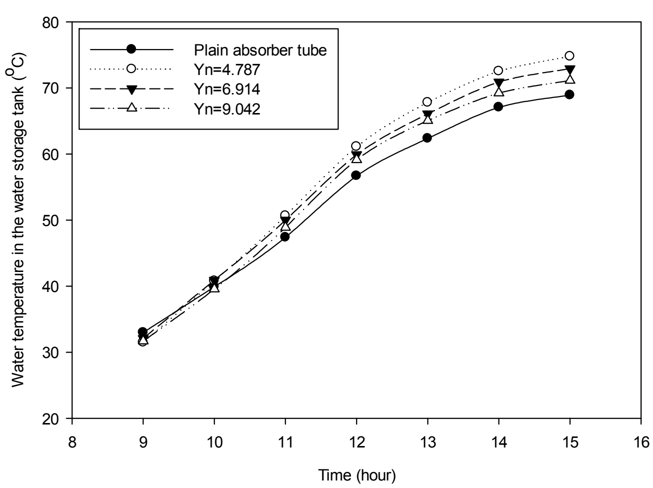

Figure 8. Variation of water temperature in the water storage tank with time and nail twist pitch ratio

Preprints (www.preprints.org) | NOT PEER-REVIEWED | Posted: 5 December 2017 doi:10.20944/preprints201712.0030.v1

Peer-reviewed version available at Energies 2018, 11, 204; doi:10.3390/en11010204

5.4 Effect of nail twist pitch ratio on hourly solar energy collected

The hourly solar energy collected vs. time has been shown in Figure 9. The hourly solar energy collected increases from 9:00 h to 11:00 h with a faster rate and reaches a peak value at noon. After noon its value again decreases and reaches a minimum value. From this figure, it is also clearly observed that hourly solar energy collected enhances with a significantly faster rate from 9:00 h to noon and after noon it begins to decay. Therefore, hourly solar energy collected follows the path of variation of incident solar radiation and useful heat gain. From the present experimental investigation, the maximum values of hourly solar energy collected are observed during the time interval between 12:00 and 13:00 h. Also, the maximum value of hourly solar energy collected has found to be increased by 12.189 % for nail twist pitch ratio 4.787, 9.770 % for nail twist pitch ratio 6.914 and 6.733 % for nail twist pitch ratio 9.042 than the same obtained from for the plain absorber tube. This is due to the matter that swirl flow and turbulent induced by the NTT inserted absorber tube. The combined effect increases the useful heat gain that in turn increases the hourly solar energy collected.

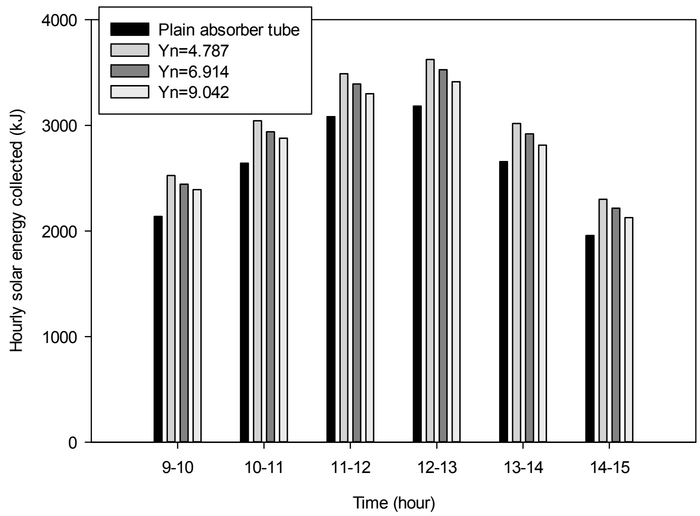

Figure 9. Variation of hourly solar energy collected with time and nail twist pitch ratio

5.5 Effect of nail twist pitch ratio on hourly solar energy stored in the water storage tank

Figure 10 shows the variation of hourly solar energy stored with nail twist pitch ratio and time. From this figure, it is very clear that hourly solar energy collected increases between the time period of 9:00 h and 13:00 h as increases the hourly solar energy collected. After that its value decreases with a faster rate till 15:00 h as the hot water is heated again and again so useful heat gain gradually decreases during this time period. Also, hourly solar energy stored increases with decreasing nail twist pitch ratio. As the lower nail twist pitch ratio strongly intensifies the swirling flow and turbulent in the absorber tube. The combined effect improves hourly solar energy stored. From the present experimental study, the maximum value of hourly solar energy stored has found to be increased by 11.087 % for nail twist pitch ratio 4.787, 6.154 % for nail twist pitch ratio 6.914 and 9.179 % for nail twist pitch ratio 9.042 than the same for plain absorber tube. Maximum values of hourly solar energy stored are observed during the time interval between 11:00 and 12:00 h.

Peer-reviewed version available at *Energies* **2018**, *11*, 204; doi:10.3390/en11010204

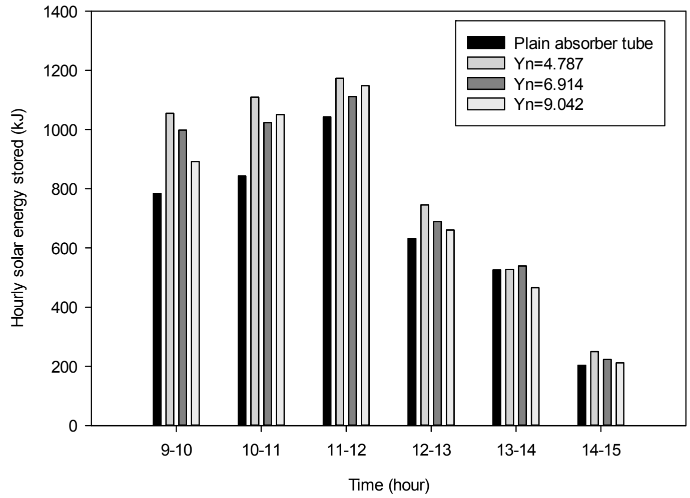

Figure 10. Variation of hourly solar energy stored with time and nail twist pitch ratio

5.6 Effect of nail twist pitch ratio on Temperature rise parameter

Figure 11 indicates the variation of temperature rise parameter with time for the nail twist pitch ratios 4.787, 6.914 and 9.042 respectively. This figure clearly shows that temperature rise parameter increases with a higher rate from 9:00 h to 11:00 h as the solar intensity increases and after that, it attains a maximum value at noon. After 13:00 h its value decreases to a minimum value with a faster rate as storage hot water is circulating through the absorber tube and this result a very little increase in water outlet temperature at the absorber tube. Therefore temperature rise parameter decreases and follows the path of variation of solar intensity. Also, the temperature rise parameter increases for NTT insert absorber tube with smaller nail twist pitch ratio. As swirl flow and turbulent created by tape twist and nail of the NTT inserts absorber tube and the smaller nail twist pitch ratio deeply intensify the swirling and turbulence. From the present experimental study, it has been observed that the maximum value of temperature rise parameter is increased by 13.168 % for nail twist pitch ratio 4.787, 11.815 % for nail twist pitch ratio 6.914 and 9.444 % for nail twist pitch ratio 9.042 than the result obtained from plain absorber tube. Therefore, NTT influences temperature rise parameter.

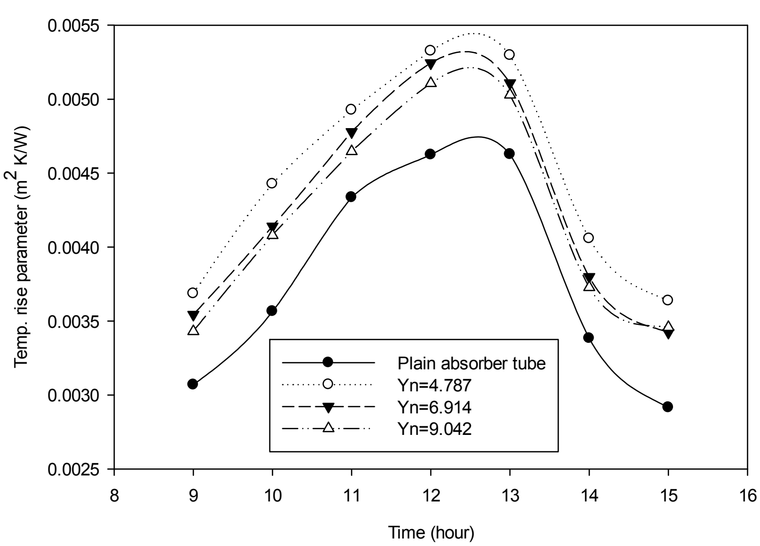

Figure 11. Variation of temperature rise parameter with time and nail twist pitch ratio

Preprints (www.preprints.org) | NOT PEER-REVIEWED | Posted: 5 December 2017 doi:10.20944/preprints201712.0030.v1

Peer-reviewed version available at Energies 2018, 11, 204; doi:10.3390/en11010204

5.7 Effect of nail twist pitch ratio on instantaneous efficiency

Figure 12 shows the change of instantaneous efficiency with time for the nail twist pitch ratios 4.787, 6.914 and 9.042. This figure shows that instantaneous efficiency rises from 9:00 h to 11:00 h and beyond this time its value rises substantially with a slower rate till noon. After this, its value decreases with time. From this experimental work, it is found that the instantaneous efficiency reaches to a peak value 64.280 % for the nail twist pitch ratio 4.787, 63.299 % for nail twist pitch ratio 6.914 and 61.639 % for the nail twist pitch ratio 10.106 at noon. The same has found to be 55.820 % for the plain absorber tube. This is due the fact that water flows through the path directed by the tape twist and turbulence magnify by the nail of the NTT inserted absorber tube, the combined effect increases in useful heat gain. Thus, increase in instantaneous efficiency.

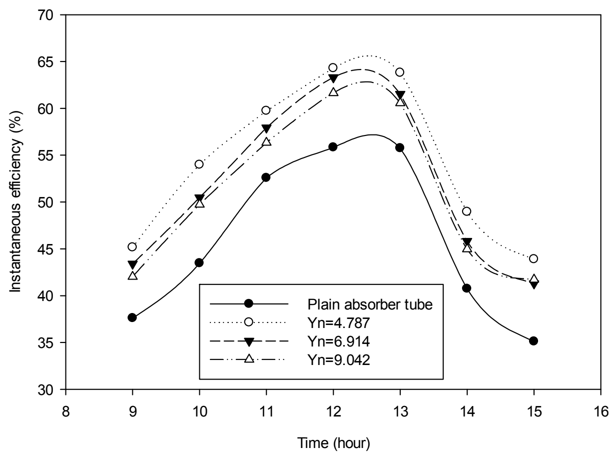

Figure 12. Variation of instantaneous efficiency with time and nail twist pitch ratio

5.8 Effect of nail twist pitch ratio on charging efficiency

Figure 13 shows the variation of charging efficiency of the CPCSWH with nail twist pitch ratio and time. In this figure, it is very transparent that at the starting of the experiment, the charging efficiency is maximum and then decreases with a slower rate from 9:00 h to 12:00 h and beyond this time it decreases with a faster rate. From this figure, it is also clear that smaller nail twist pitch ratio leads the higher charging efficiency. In case of NTT inserts in the absorber tube, swirl flow induced due to the tape twist and turbulent intensifies by the nail. This combined effect increases useful heat gain and thus increases in hourly solar energy stored in the water storage tank. From the present experimental study, the maximum overall efficiency has found to be increased by 12.489 % for nail twist pitch ratio 4.787, 10.508 % for nail twist pitch ratio 6.914 and 4.333 % for nail twist pitch ratio 9.042 than the same obtained from plain absorber tube. Therefore, the charging efficiency of the CPCSWH influenced strongly by nail twist pitch ratio and increases with decreasing nail twist pitch ratio.

Preprints (www.preprints.org) | NOT PEER-REVIEWED | Posted: 5 December 2017 doi:10.20944/preprints201712.0030.v1

Peer-reviewed version available at *Energies* **2018**, *11*, 204; doi:10.3390/en11010204

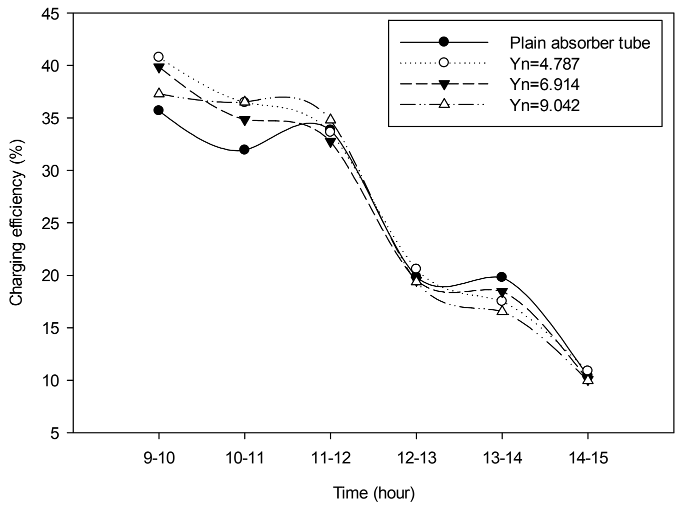

Figure 13. Variation of charging efficiency with time and nail twist pitch ratio

5.9 Effect of nail twist pitch ratio of overall thermal efficiency

Figure 14 shows the variation of overall thermal efficiency of the CPCSWH with nail twist pitch ratio and time. In this figure, it is very transparent that the overall thermal efficiency of CPCSWH increases during the first 3 h of the experiment and after this time it decreases continuously till 15:00 h. The peak values of overall thermal efficiency are observed between the time interval of 11:00 and 12:00 h. From this figure, it is also clear that smaller nail twist pitch ratio leads the higher overall thermal efficiency. It is owing to fact that the swirl flow induced by tape twist and more turbulent created by the nail of NTT. The combined effect increases the hourly solar energy stored and hence, increases the overall thermal efficiency. In the present experimental study, the maximum overall efficiency increased by 12.027 % for nail twist pitch ratio 4.787, 7.697 % for nail twist pitch ratio 6.914 and 10.697 % for nail twist pitch ratio 9.042 than the same obtained from plain absorber tube. Therefore, the overall thermal efficiency of the CPCSWH influenced by nail twist pitch ratio and the smaller nail twist pitch ratio influences strongly than the higher nail twist pitch ratio one.

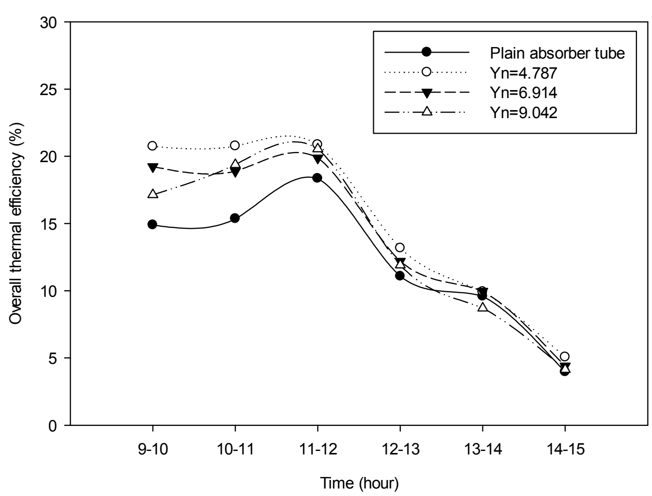

Figure 14. Variation of overall l efficiency with time and nail twist pitch ratio

doi:10.20944/preprints201712.0030.v1

Peer-reviewed version available at *Energies* **2018**, *11*, 204; doi:10.3390/en11010204

6. Conclusions

The solar intensity increases with a faster rate from 9:00 h to 11:00 h and reaches to a maximum value at noon and after noon again start to decreases.

Useful heat gain, hourly solar energy collected, temperature rise parameter and instantaneous efficiency are observed to be following the path of variation of solar intensity. The peak values of these parameters are found at noon when the solar intensity arrives a maximum. Smaller nail twist pitch ratio enhances the above-said parameters.

Water outlet temperature and water temperature in the water storage tank both increases from 9:00 h to 11:00 h with a faster rate and from 12:00 h to 15:00 h with a very slow rate. The peak value of water outlet temperature and temperature of water in the water storage tank are observed at 15:00 h.

The maximum values of hourly solar energy collected is found between 12:00 h and 13:00 h. whereas hourly solar energy stored are found to be maximum between 11:00 h and 12:00 h. Also, smaller nail twist pitch ratio leads to a higher value of hourly solar energy collected and hourly solar energy stored.

Temperature rise parameter, instantaneous efficiency and overall thermal efficiency follow the path of variation of solar intensity. At the starting of the experiment, the charging efficiency is maximum. Smaller nail twist pitch ratio causes the higher value of the above-said parameters.

.

Conflicts of Interest: The authors declare no conflict of interest.

Nomenclatures

A_f Absorber tube flow cross-sectional area (m^2)

A_{ap} Reflector aperture area (m^2)

c_p Specific heat (J kg^{-1} $^oC^{-1}$)

D_i Absorber tube inner diameter (m)

D_o Absorber tube outer diameter (m)

d_n Nail diameter (m)

E_c Hourly solar energy collected (kJ)

E_{st} Hourly solar energy stored (kJ)

I_b Solar intensity (W m^{-2})

I_h Hourly solar intensity (kJ m^{-2} h^{-1})

k_f Thermal conductivity (W m^{-1} □$^{-1}$)

l_{eff} Effective length of nail, l_{eff}=(l_n-t) (m)

l_n Length of nail (m)

L_p absorber tube length (m)

m Mass flow rate of water (kg s^{-1})

m_{st} Mass of water in the water storage tank (kg)

P Twist pitch of nail type twisted tape (m)

Q Useful heat gain (W)

t Thickness of nail type twisted tape (m)

T_b Bulk mean temperature (□)

$T_{b,st}$ Bulk mean temperature of water in the water storage tank, (^{o}C)

T_i Water inlet temperature (□)

T_o Water outlet temperature (□)

T_p Absorber tube surface temperature (□)

T_{st} Water temperature in the water storage tank (°C)

TRP Temp. rise parameter (m^2 °C W^{-1})

u_f Velocity of water (m s^{-1})

V_f Volumetric water flow rate (m^3)

w Width of nail type twisted tape (m)

Y_n Nail twist pitch ratio (P l_{eff}^{-1})

Greek Symbols

ρ_f Density of water (kg m^{-3})

η_i Instantaneous efficiency

η_{ch} Charging efficiency

η_o Overall thermal efficiency

Abbreviations

CPCSWH Cylindrical parabolic concentrating solar water heater

NTT Nail type twisted tape

PCR Parabolic concentrating reflector

Subscripts

j At any time interval

j+1 One hour time interval from j^{th} time

References

1. Huang, B.J.; Wung, T.Y.; Nieh, S. Thermal analysis of black liquid cylindrical parabolic collector. *Sol. Energy* **1979**, 22, 221-224.
2. Heiti, R.V.; Thodos, G. An experimental parabolic cylindrical concentrator: its construction and thermal performance, *Sol. Energy* **1983,** 30, 483-485.
3. Hamad, F.A.W. The performance of a cylindrical parabolic solar concentrator, *Energy Conver. Manag.* **1988,** 28, 251-256.
4. Mullick, S.C.; Nanda, S.K An improved technique for computing the heat loss factor of a tubular absorber, *Sol. Energy* **1989**, 42, 1-7.
5. Kothdiwala, A.F.; Norton, B.; Eames, P.C. The effect of variation of angle of inclination on the performance of low-concentration-ratio compound parabolic concentrating solar collectors, *Sol. Energy* **1995**, 55, 301-309.
6. Eskin, N. Transient performance analysis of cylindrical parabolic concentrating collector comparison with experimental results, *Energy Conver. Manag.* **1999**, 40, 175-191.
7. Eck, M.; Hirsch, T. Dynamics and control of parabolic trough collector loops with direct steam generation. *Sol. Energy* **2007**, 81, 268-279.
8. Kim, Y.; Han, G.; Seo, T. An evaluation on thermal performance of CPC solar collector, *Inter. Commun. in Heat and Mass Transfer* **2008**, 35, 446-457.
9. Oommen, R.; Jayaraman, S. Development and performance analysis of compound parabolic solar concentrators with reduced gap losses oversized reflector, *Energy Conver. Manag.* **2001**, 42, 1379-1399.
10. El Fadar, A.; Mimet, A.; Perez-Garcia, M. Modeling and performance study of a continuous adsorption refrigeration system driven by parabolic trough solar collector. *Sol. Energy* **2009**, 83, 850-861.
11. Padilla, R.V.; Demirkaya, G.; Goswami, D. Y.; Stefanakos, E.; Rahman, M.M. Heat transfer analysis of parabolic trough solar receiver, *Appl. Energy* **2011**, 88, 5097-5110.
12. Gang, P.; Guiqiang, L.; Xi, Z.; Jie, J.; Yuehong, S. Experimental study and exergetic analysis of a CPC-type solar water heater system using higher-temperature circulation in winter. *Sol. Energy* **2012**, 86, 1280-1286.

13. Kumaresan, G.; Sridhar, R.; Velraj, R. Performance studies of a solar parabolic trough collector with a thermal energy storage system. *Energy* **2012**, 47, 395-402.
14. Reddy, K.S.; Ravi Kumar, K. Solar collector field design and viability analysis of stand-alone parabolic trough power plants for Indian conditions, *Energy for Sustain. Develop*. **2012**, 16, 456-470.
15. Ceylan, I.; Ergun, A. Thermodynamic analysis of a new design of temperature controlled parabolic trough collector, *Energy Conver. Manag*. **2013**, 74, 505-510.
16. Syed Jafar, K; Sivaraman, B. Thermal performance of solar parabolic trough collector using nanofluid and the absorber with nail twisted tapes inserts. *Inter. Energy Journal* **2014**, 14, 189-198.
17. Mwesigye A.; Ochende, T. B.; Meyer, J.P. Minimum entropy generation due to heat transfer and fluid friction in a parabolic trough receiver with non-uniform heat flux at different rim angles and concentration ratios. *Energy* **2014**, 73, 606-617.
18. Khanna, S.; Sharma, V. Effect of number of supports on the bending of absorber tube of parabolic trough concentrator. *Energy* **2015**, 93, 1788-1803.
19. Jaramillo, O.A.; Borunda, M.; Velazquez-Lucho, K.M.; Robles, M. Parabolic trough solar collector for low enthalpy processes: An analysis of the efficiency enhancement by using twisted tape inserts. *Renew. Energy* **2016**, 93, 125-141.
20. Liang, H.; You, S.; Zhang, H. Comparison of three optical models and analysis of geometric parameters for parabolic trough solar collectors. *Energy* **2016**, 96, 37-47.
21. Fuqiang, W.; Zhexiang, T.; Xiangtao, G.; Jianyu, T.; Huaizhi, H.; Bingxi, L. Heat transfer performance enhancement and thermal strain restrain of tube receiver for parabolic trough solar collector by using asymmetric outward convex corrugated tube. *Energy* **2016**, 114, 275-292.
22. Bortolato, M.; Dugaria, S.; Col, D. D. Experimenta study of a parabolic trough solar collector with flat bar-and-plate absorber during direct steam generation. *Energy* **2016**, 116, 1039-1050.
23. Zhao, D.; Xu, E.; Zhifeng, Yu, Q.; Xu, L.; Zhu, L. Influences of installation and tracking errors on the optical performance of a solar parabolic trough collector. *Renew. Energy* **2016**, 94, 197-212.
24. Zou, B.; Dong, J.; Yao, Y.; Jiang, Y. A detailed study on the optical performance of parabolic trough solar collectors with Monte Carlo Ray Tracing method based on theoretical analysis. *Sol. Energy* **2017**, 147, 189-201.
25. Fraidenraich, N.; Filho, M. H. de O.P.; Vilela, O. de C. A new approach for obtaining angular acceptance function of non-perfect parabolic concentrating collectors. *Sol. Energy* **2017**, 147, 455-462.
26. Kline, S.J.; McKlintock, F.A. Describing uncertainties in single-sample experiments. *Mech. Engg.* **1953**, 75, 3-8.